Strontium Selenogermanate(III) and Barium Selenogermanate(II,IV): Synthesis, Crystal Structures, and Chemical Bonding

Dirk Johrendt* and Markus Tampier[a]

Abstract: The new selenogermanates $Sr_2Ge_2Se_5$ and $Ba_2Ge_2Se_5$ were synthesized by heating stoichiometric mixtures of binary selenides and the corresponding elements to 750 °C. The crystal structures were determined by single-crystal X-ray methods. Both compounds adopt previously unknown structure types. $Sr_2Ge_2Se_5$ ($P2_1/n$, $a = 8.445(2)$ Å, $b = 12.302$ Å, $c = 9.179$ Å, $\beta = 93.75(3)°$, $Z = 4$) contains $[Ge_4Se_{10}]^{8-}$ ions with homonuclear Ge–Ge bonds ($d_{Ge-Ge} = 2.432$ Å), which may be described as two ethane-like $Se_3Ge{-}GeSeSe_{2/2}$ fragments sharing two selenium atoms. $Ba_2Ge_2Se_5$ ($Pnma$, $a = 12.594(3)$ Å, $b = 9.174(2)$ Å, $c = 9.160(2)$ Å, $Z = 4$) contains $[Ge_2Se_5]^{4-}$ anions built up by two edge-sharing $GeSe_4$ tetrahedra, in which one terminal Se atom is replaced by a lone pair from the divalent germanium atom. The alkaline earth cations are arranged between the complex anions, each coordinated by eight or nine selenium atoms. $Ba_2Ge_2Se_5$ is a mixed-valence compound with Ge^{II} and Ge^{IV} coexisting within the same anion. $Sr_2Ge_2Se_5$ contains exclusively Ge^{III}. These compounds possess electronic formulations that correspond to $(Sr^{2+})_2(Ge^{3+})_2(Se^{2-})_5$ and $(Ba^{2+})_2Ge^{2+}Ge^{4+}(Se^{2-})_5$. Calculations of the electron localization function (ELF) reveal clearly both the lone pair on Ge^{II} in $Ba_2Ge_2Se_5$ and the covalent Ge–Ge bond in $Sr_2Ge_2Se_5$. Analysis of the ELF topologies shows that the Ge^{III}–Se and Ge^{IV}–Se covalent bonds are almost identical, whereas the Ge^{II}–Se interactions are weaker and more ionic in character.

Keywords: alkaline earth metals · chemical bonding · germanium · selenium · structure elucidation

Introduction

The structures of ternary and quaternary thio- and selenogermanates are characterized by tetrahedral $[GeQ_4]^{n-}$ (Q = S, Se) anions separated by electropositive transition metal and/or main-group metal cations. Thiogermanates are formally the higher homologues of silicates and a variety of structures arise by arranging and connecting the tetrahedra in space. [1–4] But in spite of their common tetrahedral motif for the anions, silicate and thio(seleno)germanate chemistries are different. The reason is the more covalent character of Ge–S(Se) bonds compared with Si–O. For instance, the *ortho* compounds A_2GeQ_4 (A = divalent metal) with isolated tetrahedra form the olivine structure (known for silicates) only if the cation A is small (as for transition metals, Mg, and Ca).[5,6] Otherwise special structure types emerge that are not known in silicates.[7] Corner sharing of the tetrahedra leads to *meta* compounds with infinite ${}^1_\infty[GeQ_4]^{2-}$ chains. Examples are Na_2GeS_3[8] or the recently described $PdGeS_3$.[9] Oligomeric anions $[Ge_2S_7]^{6-}$ (corner sharing), $[Ge_2S_6]^{4-}$ (edge sharing), or the adamatane-like $[Ge_4S_{10}]^{4-}$ were also reported, the last of which were also obtained from aqueous solutions.[10–13] Larger oligomeric anions are known for the cesium selenogallates(III) $Cs_{n+4}[Ga_nSe_{2n+2}]$ with $n = 2–6$.[14,15]

Nearly all of the known compounds fulfil electronically precise ionic formulations if assumed to contain Ge^{IV}, for example, $(Mg^{2+})_2Ge^{4+}(S^{2-})_4$, $Pd^{2+}Ge^{4+}(S^{2-})_3$, or $(Ba^{2+})_2(Cu^{1+})_6(Ge^{4+})_2(S^{2-})_8$. They are often intensely colored and are expected to be semiconducting, in contrast to the insulating silicates. Unfortunately, the physical properties of thio- and selenogermanates have scarcely been investigated up to now.

Germanium compounds with tetrahedral chalcogen coordination contain exclusively Ge^{IV}. The stability of lower oxidation states increases within Group 14 from carbon to lead. Carbon and silicon exist in chalcogenides as C^{IV} and Si^{IV}, while lead is found exclusively as Pb^{II}, and tin is stable as Sn^{II} and Sn^{IV}. Silicon and germanium clearly prefer to be tetravalent, but lower oxidation states are possible. Examples are the binary compounds GeQ (Q = S, Se) with Ge^{II}.[16] The presence of homonuclear Ge–Ge bonds (that is, Ge^{III}) is assumed in the glassy Ge_2Q_3 (Q = S, Se).[17] Until now, ternary Ge^{III} compounds have existed only with alkaline metals: the thio-, seleno-, and tellurogermanates(III) $A_6Ge_2Q_6$ (A = K, Na, Q = S, Se, Te) contain $[Ge_2Q_6]^{6-}$ units with covalent Ge–Ge bonds.[18] The homologous tellurosilicate(III) $K_6Si_2Te_6$ and tellurostannate(III) $K_6Sn_2Te_6$ are also known.[19,20] Like-

---

[a] Dr. D. Johrendt, M. Tampier
Institut für Anorganische Chemie und Strukturchemie II
der Heinrich-Heine-Universität Düsseldorf
Universitätsstrasse 1, 40225 Düsseldorf (Germany)
Fax: (+49) 211-811-4146
E-mail: johrendt@uni-duesseldorf.de

0947-6539/00/0606-0994 $ 17.50+.50/0

wise, Ge^{III} was observed in the cyclic $[(GeTe_2)_4Te_2]^{8-}$ anion of $Na_8Ge_4Te_{10}$.[21] Divalent Ge^{II} coexists with Ge^{IV} in $Tl_2Ge_2S_4$ to form infinite $^1_\infty[Ge^{II}{}_2Ge^{IV}{}_2S_8]^{4-}$ chains.[22]

In our investigations into ternary and quaternary selenogermanates of the alkaline earth metals, we have found two new compounds of the type $A_2Ge_2Se_5$ (A = Sr, Ba). Although of the same formula type, they adopt different crystal structures and contain germanium in the oxidation states (III) and (II)/(IV), respectively. In this paper, we report the synthesis, crystal structures, and chemical bonding of $Sr_2Ge_2Se_5$ and $Ba_2Ge_2Se_5$.

Results and Discussion

Crystals of $Sr_2Ge_2Se_5$ are amber but transparent and show no reaction when exposed to air or water. The compound crystallizes in a previously unknown monoclinic structure type with four formula units per unit cell. The structure is shown in Figure 1; selected atomic bond lengths and angles are given in Table 1.

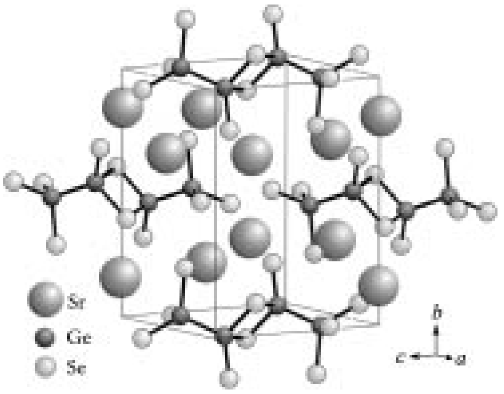

Figure 1. Crystal structure of $Sr_2Ge_2Se_5$.

Table 1. Selected bond lengths [Å] and angles [°] for $Sr_2Ge_2Se_5$.

Sr1–Se2	3.117(3)	Sr2–Se3	3.065(3)	Ge1–Se5	2.324(3)
Sr1–Se1	3.197(3)	Sr2–Se2	3.094(3)	Ge1–Se4	2.380(3)
Sr1–Se4	3.217(3)	Sr2–Se3	3.188(3)	Ge1–Se4	2.446(3)
Sr1–Se5	3.220(3)	Sr2–Se2	3.247(3)	Ge1–Ge2	2.432(3)
Sr1–Se3	3.316(3)	Sr2–Se5	3.308(3)	Ge2–Se1	2.316(3)
Sr1–Se5	3.331(3)	Sr2–Se1	3.325(3)	Ge2–Se2	2.355(3)
Sr1–Se1	3.440(3)	Sr2–Se5	3.379(3)	Ge2–Se3	2.381(3)
Sr1–Se3	3.541(3)	Sr2–Se4	3.688(3)	Ge2–Ge1	2.432(3)
Se5-Ge1-Se4	117.8(1)	Se4-Ge1-Ge2	99.0(1)	Se1-Ge2-Ge1	114.8(1)
Se5-Ge1-Ge2	124.2(1)	Se4-Ge1-Se4	95.2(1)	Se2-Ge2-Se3	99.6(1)
Se5-Ge1-Se4	107.5(1)	Se1-Ge2-Se2	103.1(1)	Se2-Ge2-Ge1	114.8(1)
Se4-Ge1-Ge2	113.6(1)	Se1-Ge2-Se3	118.4(1)	Se3-Ge2-Ge1	105.5(1)

The most striking feature of $Sr_2Ge_2Se_5$ is its isolated $[Ge_4Se_{10}]^{8-}$ anions. They are oriented roughly along [101], separated and balanced in terms of charge by Sr^{2+} cations. Sr1 is coordinated by eight selenium atoms to form a distorted bicapped trigonal prism. Sr2 has a distorted quadratic-antiprismatic coordination with one more Se over a quadratic plane. The germanium is four-coordinate—three selenium and one germanium atom form a distorted tetrahedron (angles ≈ 100 – 118°). Figure 2 shows some geometric details of the centrosymmetric $[Ge_4Se_{10}]^{8-}$ anion. The coordination of germanium remains tetrahedral as in $[GeSe_4]^{4-}$, but one neighbor is now Ge instead of Se. Evidently, the Ge–Se bonds are not significantly influenced by this fact. The Ge–Se distances range from 2.32 to 2.45 Å and correspond approximately to the sum of the covalent radii (2.36 Å),[23] as found for other selenogermanates with tetrahedral $GeSe_4$ units.[24] Each of the two Ge–Ge dumbbells ($d_{Ge-Ge} = 2.432$ Å) is bridged by two Se atoms. A four-membered ring is formed by two Ge and the two common Se atoms. The $[Ge_4Se_{10}]^{8-}$ anion may be regarded as two ethane-like $Se_3Ge–GeSeSe_{2/2}$ fragments sharing two selenium atoms. As mentioned above, isolated $[Ge_2Se_6]^{6-}$ anions have been observed in $K_6Ge_2Se_6$,[18] in which the $Se_3Ge–GeSe_3$ groups adopt a "staggered" conformation as expected by lone-pair repulsion arguments.

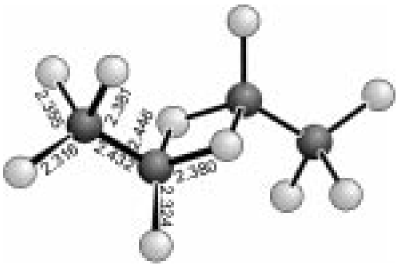

Figure 2. $[Ge_4Se_{10}]^{8-}$ anion of $Sr_2Ge_2Se_5$.

Abstract in German: *Die neuen Selenogermanate $Sr_2Ge_2Se_5$ und $Ba_2Ge_2Se_5$ wurden durch Erhitzen stöchiometrischer Gemenge aus Erdalkaliseleniden und den Elementen auf 750°C dargestellt und ihre Kristallstrukturen röntgenographisch mit Einkristallmethoden bestimmt. Beide Verbindungen bilden bisher unbekannte Strukturtypen. $Sr_2Ge_2Se_5$ kristallisiert monoklin ($P2_1/n$, $a = 8.445(2)$ Å, $b = 12.302$ Å, $c = 9.179$ Å, $\beta = 93.75(3)°$, $Z = 4$); wesentliches Strukturmerkmal sind isolierte $[Ge_8Se_{10}]^{8-}$-Anionen mit homonuklearen Ge–Ge Bindungen. Das Anion besteht aus zwei kondensierten ethananalogen $Se_3Ge–GeSeSe_{2/2}$-Fragmenten mit zwei verbrückenden Se-Atomen. $Ba_2Ge_2Se_5$ ($Pnma$, $a = 12.594(3)$ Å, $b = 9.174(2)$ Å, $c = 9.160(2)$ Å, $Z = 4$) dagegen bildet neuartige $[Ge_2Se_5]^{4-}$-Anionen. Sie leiten sich von kantenverknüpften Ge_2Se_6-Doppeltetraedern ab, indem ein Se-Atom durch das einsame Elektronenpaar eines Ge^{II} ersetzt wird. Die Erdalkaliatome sind in beiden Fällen acht- oder neunfach von Selen koordiniert. $Ba_2Ge_2Se_5$ ist eine gemischtvalente Verbindung, in der Ge^{II} und Ge^{IV} gleichzeitig in einem komplexen Anion vorliegen. $Sr_2Ge_2Se_5$ enthält ausschließlich Ge^{III}. Beide Selenogermanate sind elektrovalent aufgebaut, entsprechend den ionischen Formulierungen $(Sr^{2+})_2(Ge^{3+})_2(Se^{2-})_5$ und $(Ba^{2+})_2Ge^{2+}Ge^{4+}(Se^{2-})_5$. Die Elektronenlokalisierungsfunktion ELF zeigt deutlich das einsame Elektronenpaar des Ge^{II} in $Ba_2Ge_2Se_5$ und die kovalente Ge–Ge Bindung in $Sr_2Ge_2Se_5$. Eine Analyse der ELF-Topologie ergibt weiterhin, dass sich kovalente Ge^{III}–Se und Ge^{IV}–Se Bindungen praktisch nicht unterscheiden, während die Ge^{II}–Se Wechselwirkung in $Ba_2Ge_2Se_5$ schwächer ist und deutlich ionischen Charakter aufweist.*

In contrast to this, the conformation of the $Se_3Ge{-}GeSeSe_{2/2}$ groups in $Sr_2Ge_2Se_5$ is almost "eclipsed" with a Se–Se distance of 4.74 Å, that is, longer than twice the van der Waals radius of Se (2.0 Å).[25] Thus, this is an arrangement of low energy, because if the terminal $GeSe_3$ group were rotated by 180° around the Ge–Ge bond to reach a "staggered" conformation, the distance to the terminal Se atoms of the *neighboring* $GeSeSe_{2/2}$ group would be only 4.38 Å. Consequently the repulsive energy would be even higher. However, the observed conformation depends also substantially on packing and on the coordination requirements of the Sr^{2+} cations and is not a result of lone-pair repulsion forces alone.

Owing to the formation of Ge–Ge bonds, the formal oxidation state of germanium in $Sr_2Ge_2Se_5$ is Ge^{III}. This leads to an electronically precise ionic formula of $(Sr^{2+})_2(Ge^{3+})_2(Se^{2-})_5$ in agreement with the color and transparency of the crystals.

The deep red crystals of $Ba_2Ge_2Se_5$ are transparent only in very thin layers and stable when exposed to air or humidity. The compound adopts a novel orthorhombic structure type in the space group *Pnma*. Selected atomic distances and angles are compiled in Table 2. As seen in Figure 3, we find isolated complex anions built up by Ge and Se, but in contrast to the $[Ge_4Se_{10}]^{8-}$ units in $Sr_2Ge_2Se_5$, the analogous barium compound forms $[Ge_2Se_5]^{4-}$ anions. Barium is coordinated by eight selenium atoms to form a bicapped trigonal prism. The $[Ge_2Se_5]^{4-}$ groups are aligned roughly along [001] and occur along [100] every half translation, each rotated by 180° and shifted by ½ along [010].

Table 2. Selected bond lengths [Å] and angles [°] for $Ba_2Ge_2Se_5$.

Ba–Se1	3.350(1)	Ge1–Se4	2.325(2)	Se4-Ge1-Se1	108.7(1)
Ba–Se3	3.371(1)	Ge1–Se1	2.356(2)	Se4-Ge1-Se2	110.3(1)2 ×
Ba–Se2	3.385(2)	Ge1–Se2	2.359(1)2 ×	Se1-Ge1-Se2	110.4(1)2 ×
Ba–Se4	3.394(1)	Ge2–Se3	2.443(3)	Se2-Ge1-Se2	106.8(1)
Ba–Se4	3.408(1)	Ge2–Se2	2.672(2)2 ×	Se3-Ge2-Se2	97.5(1)2 ×
Ba–Se3	3.417(1)			Se2-Ge2-Se2	90.3(1)
Ba–Se1	3.424(1)				
Ba–Se2	3.527(1)				

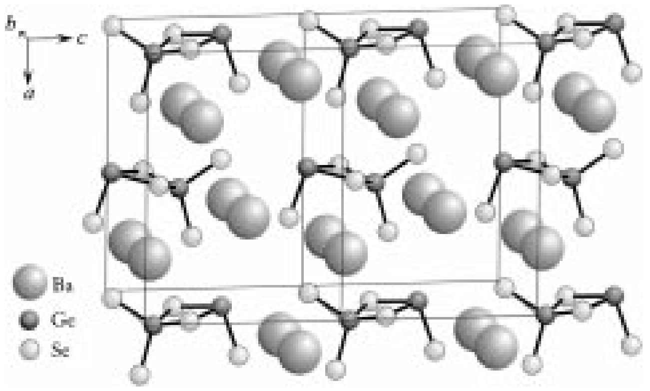

Figure 3. Crystal structure of $Ba_2Ge_2Se_5$.

Details of the complex anion $[Ge_2Se_5]^{4-}$ are given in Figure 4. It can be interpreted as two edge-sharing $GeSe_4$ tetrahedra, in which one terminal Se atom is missing and is replaced by a lone pair from the divalent germanium atom. As expected, the lower valence state of germanium produces elongated Ge–Se bonds. Compared with the Ge–Se bond lengths in binary GeSe (2.56–2.57 Å),[16] we find a shorter bond Ge^{II}–Se (2.44 Å) to the terminal selenium, but the bond lengths to the bridging selenium are longer (2.67 Å) in $[Ge_2Se_5]^{4-}$. The Ge^{IV}–Se bond lengths are 2.33–2.36 Å and correspond approximately to the sum of the covalent radii of Ge and Se (2.36 Å).[23] This indicates that Ge–Se bonds for Ge in tetrahedral coordination are not influenced by changing one neighbor from Se to Ge as in $Sr_2Ge_2Se_5$, but we find significant differences when one atom is "replaced" by a lone pair in $Ba_2Ge_2Se_5$.

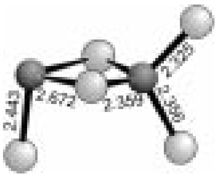

Figure 4. $[Ge_2Se_5]^{4-}$ anion of $Ba_2Ge_2Se_5$.

$Ba_2Ge_2Se_5$ is a mixed-valence compound. Divalent Ge^{II} and tetravalent Ge^{IV} coexist within the same complex anion. As in $Sr_2Ge_2Se_5$ with its exclusively trivalent Ge^{III}, the ionic formula splitting for $Ba_2Ge_2Se_5$ results in an electronically precise formulation, namely $(Ba^{2+})_2Ge^{2+}Ge^{4+}(Se^{2-})_5$. In a crystal structure built up from isolated anions as found in $Sr_2Ge_2Se_5$, no drastic change is expected when strontium is replaced by barium. Particularly the anions should be the same; merely the distances between them may be increased because of the larger ionic radius of barium compared with strontium. However, the question of why $Ba_2Ge_2Se_5$ and $Sr_2Ge_2Se_5$ form such different complex anions must remain open.

The electronic structure of $Sr_2Ge_2Se_5$ and $Ba_2Ge_2Se_5$ was investigated by means of non-empirical band structure calculations. As expected from the electron-precise compositions, both compounds turn out to be semiconductors. The calculated band gaps are 1.2 eV for $Sr_2Ge_2Se_5$ and 1.6 eV for $Ba_2Ge_2Se_5$. However, it must be kept in mind that density functional calculations always produce too small gaps compared with experimental values.

In order to visualize the chemical bonding in $Sr_2Ge_2Se_5$ and $Ba_2Ge_2Se_5$, we have calculated the electron localization function (ELF) for selected planes within the anions $[Ge_4Se_{10}]^{8-}$ and $[Ge_2Se_5]^{4-}$. The values of ELF are defined between zero and one; large values (>0.7) mean a high probability of paired electron spins, that is, regions of either covalent bonds or lone pairs of electrons. Local maxima of the ELF define localization attractors. The valence-electron ELF maps (core states are not considered) in Figures 5 and 6 render contour lines from $ELF = 0.5$ to $ELF = 0.95$ with increments of 0.05.

Figure 5 shows the ELF contours of a plane within the $[Ge_4Se_{10}]^{4-}$ anion of $Sr_2Ge_2Se_5$. The attractor of the covalent Ge–Ge bond can be clearly discerned and is not completely symmetric because of the different kinds of surrounding selenium atoms. Ge1 is connected to two bridging Se4 and one terminal Se5 (not within the plane), whereas the neighbors of Ge2 are exclusively terminal atoms Se1–3. Areas of high ELF

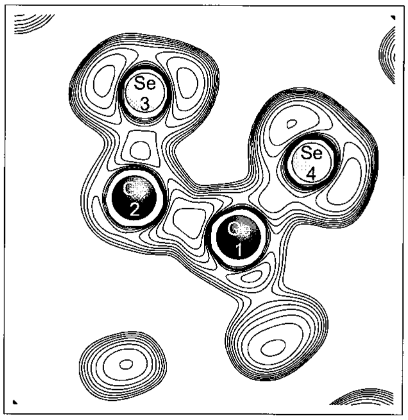

Figure 5. Electron localization function (ELF) of $[Ge_4Se_{10}]^{8-}$. (Contours are from 0.5 to 0.95 with increments of 0.05.)

are also seen in the Ge–Se bonding regions and around the selenium atoms, these latter regions correspond to the lone pairs of Se and reach values up to ELF = 0.9. In seleno- and thiogermanate compounds, one generally observes shorter bonds between germanium and the terminally bonded chalcogens compared with bridging ones[1]. The ELF topology of $[Ge_4Se_{10}]^{8-}$ reveals this small difference. Even if the distances Ge1–Se4 (bridging) and Ge2–Se3 (terminal) are nearly identical 2.38 Å, we still see the bonding attractor (bound by ELF $\approx$ 0.8) between Ge2 and Se3, which is shifted slightly towards the germanium atom. In the bonding region between Ge1 and Se4, the ELF reaches also values of about 0.8, but the attractor is more spread out in space. This indicates weaker bonding to the bridging selenium atom compared with the terminal one.

Figure 6 shows the ELF contours of the $[Ge_2Se_5]^{4-}$ ion. The highest values (up to 0.97) are seen in the vicinity of the Ge2 atom. This is the strongly localized lone pair of electrons of divalent Ge^{II}. It does not point directly to a neighboring Ba^{2+}, but rather towards empty space (see Figure 3). The ELF topology for the $[Ge_2Se_5]^{4-}$ anion in $Ba_2Ge_2Se_5$ reveals the differences between Ge^{IV}–Se and Ge^{II}–Se bonding. The Ge1–Se4 and Ge1–Se2 (each Ge^{IV} to terminal Se) bonds represent the typical case expected for tetravalent germanium compounds. All bonding attractors are bound with values of ELF $\approx$ 0.8 between Ge and Se and nearly 0.9 in the areas of the selenium lone pairs. As mentioned above, the Ge(III)–Se bonds in $Sr_2Ge_2Se_5$ (compare with Ge2–Se3 in Figure 5) are practically identical with the Ge^{IV}–Se in $Ba_2Ge_2Se_5$.

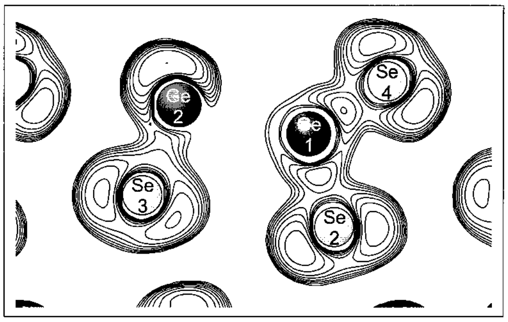

Figure 6. Electron localization function (ELF) of $[Ge_2Se_5]^{4-}$.

In contrast to this, we see no sharply bound ELF attractor between Ge2 (which is Ge^{II}) and Se3. The ELF values are lower (about 0.7) and the topology is more spherical around Se3. From this we can conclude, that the Ge^{II}–Se bonds are weaker and have more ionic character compared with covalent Ge^{IV}–Se bonds. Increasing ionicity results in longer Ge–Se distances, as seen from the NaCl type high-temperature phase of GeSe, in which the germanium has six neighboring selenium atoms with bond lengths of 2.865 Å.[26] In $Ba_2Ge_2Se_5$ we observe the previously unprecedented case of the coexistence of almost covalent Ge^{IV}–Se and ionic Ge^{II}–Se bonding within the same isolated anion.

Experimental Section

General: Starting materials were selenium powder (Alfa, 99.999 %), germanium powder (Chempur, 99.999 %), SeO_2 (Merck, 99.99 %), $BaCl_2$, and $SrCl_2$ (Merck, 99.9 %).

Barium selenide and strontium selenide (BaSe and SrSe): Solutions of $BaCl_2$ and SeO_2 (each 0.2 mol l^{-1}) were mixed and $BaSeO_3$ was precipitated at pH = 8. The selenite was washed and dried in vacuo before being reduced by a flow of NH_3 at 860 °C over 4 h to yield a colorless powder of BaSe. The same procedure was used to synthesize SrSe.

Strontium selenogermanate(III), $Sr_2Ge_2Se_5$ (1): A stoichiometric mixture of SrSe (0.3332 g, 2 mmol), Ge (0.1452 g, 2 mmol), and Se (0.2369 g, 3 mmol) was loaded into a corundum crucible. The crucible was transferred into a silica tube and evacuated. It was flushed three times with argon before being sealed under an argon atmosphere (ambient pressure). The mixture was heated to 750 °C at a rate of 50 °C h^{-1} and was kept at this temperature for 50 h; the furnace was then allowed to cool to RT. The first product was homogenized in an argon-filled glove-box, reloaded to the crucible and subsequently tempered at 750 °C for 50 h. This procedure yielded a brown powder of $Sr_2Ge_2Se_5$, which is stable in air and insoluble in water and common organic solvents. Single crystals suitable for X-ray experiments were selected directly from the powder. No impurities could be detected within the accuracy of the X-ray powder diffraction experiment.

Barium selenogermanate(II, IV), $Ba_2Ge_2Se_5$ (2): BaSe (0.4326 g, 2 mmol), Ge (0.1452 g, 2 mmol), and Se (0.2369 g, 3 mmol) were heated as described above for compound **1**. The deep red powder showed no reaction when exposed to air or water. Small, red single crystals were transparent only as thin layers. X-ray powder patterns were indexed completely with the data obtained from the single-crystal experiment.

Structure determination: The crystal structures were determined by means of single-crystal X-ray diffraction at RT. A STOE AED-2 diffractometer was used for the data collections. Lorentz and polarization corrections were performed, absorption effects were corrected empirically by acquiring Ψ-scans. The structures were solved in the centrosymmetric space groups $P2_1/n$ ($Sr_2Ge_2Se_5$) and $Pnma$ ($Ba_2Ge_2Se_5$) by direct methods (SHELXTL)[27] and refined against F_o^2 (SHELXL-93).[28] Final refinements included anisotropic displacement parameters for all atoms. Details of the data collections and refinements are given in Table 3; the final atomic and equivalent displacement parameters are listed in Tables 4 and 5. Important interatomic distances and angles are summarized in Tables 1 and 2 for $Sr_2Ge_2Se_5$ and $Ba_2Ge_2Se_5$, respectively. Further details on the crystal structure investigations may be obtained from the Fachinformationszentrum Karlsruhe, D-76344 Eggenstein-Leopoldshafen, Germany (fax: (+49) 7247-808-666; e-mail: crysdata@fiz-karlsruhe.de), on quoting the depository numbers CSD-410790 for $Sr_2Ge_2Se_5$ and CSD-410791 for $Ba_2Ge_2Se_5$.

Electronic structure calculations: Self-consistent ab initio band structure calculations were performed with the LMTO method in its scalar relativistic version (program LMTO-ASA 47).[29] A detailed description may be found elsewhere.[30–34] Reciprocal space integrations were performed with the tetrahedron method by using 54 ($Sr_2Ge_2Se_5$) and 27 ($Ba_2Ge_2Se_5$) irreducible k-points within the Brillouin zone.[35] The basis sets consisted of 5s/5p orbitals for Sr, 6s/6p for Ba, and 4s/4p for Ge and Se. The 4d orbitals for Ge and Se were treated by the downfolding

Table 3. Crystallographic data and details of the data collection for $Sr_2Ge_2Se_5$ and $Ba_2Ge_2Se_5$.

	$Sr_2Ge_2Se_5$	$Ba_2Ge_2Se_5$
M_w	715.88	814.66
crystal system	monoclinic	orthorhombic
space group	$P2_1/n$	$Pnma$
a [Å]	8.445(2)	12.594(3)
b [Å]	12.302(2)	9.174(2)
c [Å]	9.179(2)	9.160(2)
β [°]	93.75(3)	
V [Å^3]	951.6(3)	1058.3(4)
Z	4	4
ρ_{calcd} [g cm^{-3}]	4.992	5.113
$\mu(Mo_{K\alpha})$ [mm^{-1}]	36.45	30.09
absorption correction	ψ-scans	ψ-scans
min/max transmission	0.21/0.74	0.29/0.74
diffractometer	STOE AED-2	STOE AED-2
radiation	$Mo_{K\alpha}$	$Mo_{K\alpha}$
monochromator	graphite	graphite
2θ-range [°]	3–70	3–65
index ranges	$-6 \leq h \leq 13$	$0 \leq h \leq 18$
	$-11 \leq k \leq 17$	$-13 \leq k \leq 0$
	$0 \leq l \leq 13$	$0 \leq l \leq 13$
reflections collected	8079	4406
unique reflections	4360 ($R_{int} = 0.077$)	2203 ($R_{int} = 0.057$)
observed reflections [$I > 2\sigma(I)$]	1794	1346
parameters	83	50
R_1	0.057	0.041
wR_2	0.076	0.102
goodness-of-fit	1.163	1.068
residual electron density [e Å^{-3}]	+1.75/−1.75	+3.58/−3.34

Table 4. Atomic coordinates and equivalent displacement parameters[a] for $Sr_2Ge_2Se_5$.

Atom	Position	x	y	z	U_{eq}
Sr1	4e	0.0448(3)	0.1627(1)	0.0323(2)	0.0142(5)
Sr2	4e	0.5605(3)	0.3032(2)	0.0218(2)	0.0148(5)
Ge1	4e	0.4951(3)	0.0505(2)	0.3358(3)	0.0098(5)
Ge2	4e	0.7996(3)	0.4809(2)	0.3129(2)	0.0093(5)
Se1	4e	0.2032(3)	0.4427(2)	0.4567(3)	0.0132(5)
Se2	4e	0.5380(2)	0.5082(2)	0.2145(2)	0.0119(5)
Se3	4e	0.3144(3)	0.2118(2)	0.7937(2)	0.0120(5)
Se4	4e	0.1583(2)	0.4118(2)	0.0602(2)	0.0123(5)
Se5	4e	0.3449(3)	0.2050(2)	0.2797(2)	0.0118(5)

[a] The equivalent displacement parameter is defined as one-third of the orthogonalized U_{ij} tensor.

Table 5. Atomic coordinates and equivalent displacement parameters for $Ba_2Ge_2Se_5$.

Atom	Position	x	y	z	U_{eq}
Ba	8d	0.3223(1)	0.9950(1)	0.3790(1)	0.0122(2)
Ge1	4c	0.4030(1)	¼	0.6821(2)	0.0095(3)
Ge2	4c	0.9661(1)	¼	0.4711(2)	0.0156(4)
Se1	4c	0.2225(1)	¼	0.6149(2)	0.0117(3)
Se2	8d	0.4422(1)	0.0436(1)	0.8258(1)	0.0133(2)
Se3	4c	0.2836(1)	¼	0.1193(2)	0.0129(3)
Se4	4c	0.0059(1)	¼	0.0287(2)	0.0121(3)

technique.[36] To achieve space filling within the atomic sphere approximation, interstitial spheres were introduced to avoid too large an overlap of the atom-centered spheres. The empty sphere positions and radii were calculated by using an automatic procedure developed by Krier.[37] We did not allow an overlap of more than 15% for any two atom-centered spheres. Two-dimensional grids of the electron localization function (ELF)[38] were calculated. Within density functional theory, ELF depends on the excess of local kinetic energy owing to the Pauli principle compared with the bosonic system (Pauli kinetic energy $t_{P(r)}$). By definition the values for ELF are confined to to the range 0–1. Regions in space for which the Pauli principle does not increase the kinetic energy of the electrons (i.e., high values of ELF) can be identified as areas in which pairing of electrons with opposite spins play an important role. Thus, high values of ELF can be treated as equivalent to covalent bonds or lone pairs.[39]

Acknowledgments

We are indebted to Prof. A. Mewis and Prof. D. Mootz for fruitful discussions and financial support of this work.

---

[1] J. Olivier-Fourcade, J. C. Dumas, M. Ribes, E. Philippot, *J. Solid State Chem.* **1978**, *23*, 155.
[2] B. Krebs, *Angew. Chem.* **1983**, *95*, 113; *Angew. Chem. Int. Ed. Engl.* **1983**, *22*, 13.
[3] M. Tampier, D. Johrendt, *Z. Naturforsch. Teil B* **1998**, *53*, 1483.
[4] D. Johrendt, *Z. Anorg. Allg. Chem.* **1998**, *624*, 952.
[5] H. Vincent, E. F. Bertaut, W. H. Baur, R. D. Shannon, *Acta Crystallogr. Sect. B* **1976**, *32*, 1749.
[6] T. Duc, H. Vincent, E. F. Bertaut, Vu Van Qui, *Solid State Commun.* **1969**, *7*, 641.
[7] G. Eulenberger, D. Müller, *Z. Naturforsch. Teil B* **1974**, *29*, 118.
[8] J. Olivier-Fourcade, E. Philippot, M. Ribes, M. Maurin, *Rev. Chim. Miner.* **1972**, 9, 757.
[9] D. Johrendt, M. Tampier, *Chem. Eur. J.* **1998**, *9*, 1829.
[10] J. C. Dumas, J. Olivier-Fourcade, F. Vermot-Gaud-Daniel, M. Ribes, E. Philippot, M. Maurin, *Rev. Chim. Miner.* **1974**, *11*, 13.
[11] B. Krebs, S. Pohl, W. Schiwy, *Z. Anorg. Allg. Chem.* **1972**, *393*, 241.
[12] B. Krebs, S. Pohl, *Z. Naturforsch. Teil B* **1971**, *26*, 853.
[13] C.-W. Park, M. A. Pell, J. Ibers, *Inorg. Chem.* **1996**, *35*, 4555.
[14] H.-J. Deiseroth, H. Fu-Son, *Angew. Chem.* **1981**, *93*, 1011; *Angew. Chem. Int. Ed. Engl.* **1981**, *20*, 962.
[15] H. J. Deiseroth, *Z. Kristallogr.* **1984**, *166*, 183.
[16] H. Wiedemeyer, H. G. von Schnering, *Z. Kristallogr.* **1978**, *148*, 295.
[17] A. Feltz, W. Burckhardt, L. Senf, B. Voigt, K. Zickmüller, *Z. Anorg. Allg. Chem.* **1977**, *435*, 172.
[18] B. Eisenmann, E. Kieselbach, H. Schäfer, H. Schrod, *Z. Anorg. Allg. Chem.* **1984**, *516*, 49.
[19] G. Dittmar, *Acta Crystallogr. Sect. B* **1978**, *34*, 2390.
[20] G. Dittmar, *Z. Anorg. Allg. Chem.* **1978**, *453*, 68.
[21] B. Eisenmann, H. Schäfer, H. Schwerer, *Z. Naturforsch. Teil B* **1983**, *38*, 924.
[22] G. Eulenberger, *J. Less-Common Met.* **1985**, *108*, 65.
[23] L. Pauling, *Die Natur der Chemischen Bindung*, 3rd ed., VCH, Weinheim, **1968**, p. 237.
[24] D. Johrendt, Universität Düsseldorf, unpublished results
[25] L. Pauling, *Die Natur der Chemischen Bindung*, 3rd ed., VCH, Weinheim, **1968**, p. 249.
[26] H. Wiedermeier, P. A. Siemers, *Z. Anorg. Allg. Chem.* **1975**, *411*, 90.
[27] Structure Determination System, *SHELXTL-PLUS*, Rev. 4.21/V, Siemens Analytical X-Ray Instruments Inc. Madison, WI, USA, **1990**.
[28] G. M. Sheldrick, *SHELXL-93 Progam for Crystal Structure Refinement*, Universität Göttingen, **1993**.
[29] O. K. Andersen, *Tight-Binding LMTO Vers. 47*, Max-Planck-Institut für Festkörperforschung, Stuttgart, **1994**.
[30] O. K. Andersen, *Phys. Rev.* **1975**, *B12*, 3060.
[31] O. Jepsen, O. K. Andersen, *Phys. Rev. Lett.* **1984**, *53*, 2571.
[32] O. K. Andersen, O. Jepsen, *Z. Phys.* **1995**, *B97*, 35.
[33] H. L. Skriver, *The LMTO Method*, Springer, Berlin, **1984**.
[34] O. Jepsen, M. Snob, O. K. Andersen, *Linearized Band-Structure Methods in Electronic Band-Structure and its Applications*, Springer Lecture Notes, Springer, Berlin, **1987**.
[35] O. K. Andersen, O. Jepsen, *Solid State Commun.* **1971**, *9*, 1763.
[36] W. R. L. Lambrecht, O. K. Andersen, *Phys. Rev. B* **1986**, *34*, 2439.
[37] G. Krier, O. Jepsen, O. K. Andersen, unpublished results.
[38] A. Savin, B. Silvi, *Nature* **1994**, *371*, 683.
[39] A. Savin, T. F. Fässler, *Chem. Unserer Zeit* **1997**, *31*, 110.

Received: August 19, 1999 [F1989]